JOURNAL OF APPLIED ELECTROCHEMISTRY 2 (1972) 239-249

REVIEW

Proton migration in solids

J. BRUININK

Inorganic Chemistry Department, State University of Utrecht, The Netherlands

Received 14 January 1972

Experimental methods which are suitable for the study of proton migration in solids are discussed. Special attention is paid to the determination of the transport numbers of protons. A survey is given of the relevant properties of most materials for which proton migration has been claimed.

1. Introduction

The mechanism of proton migration and the dielectric properties of hydrogen bonded materials have received considerable attention for a number of years. Ice especially has been the subject of many investigations. Knowledge of the transport properties in hydrogen bonded materials is of major importance for the understanding of many biophysical processes in biological systems [22]. Solid electrolytes with fast proton conduction could be of great interest for the construction of fuel cells. The proton conductor can be seen as the cationic equivalent of oxygen conductors. Hydrogen bonds occur in most of the crystalline solids containing hydrogen [1]. Examination of structures of different proton conductors demonstrates that the protons of these compounds are involved in hydrogen bonds, e.g. imidazole, acid salts, ice, hydrates. A remarkable exception in connection with previously mentioned compounds is ammonium chloride in which protons partake in the conduction process, but in which the proton is not hydrogen bonded [2]. Another category are materials containing hydrogen as a solid solution, e.g. $CaZrO_2H$.

In these materials no proton conduction has been demonstrated unambiguously, although some experiments reveal that it is not unreasonable to expect it here [3].

We can roughly divide hydrogen bonded solids into four groups [1]. In these groups the hydrogen bond is ordered in:

(1) Finite groups: potassium hydrofluoride.
(2) Infinite chains: β-oxalic acid, imidazole.
(3) Infinite layers: α-oxalic acid, boric acid.
(4) Infinite three-dimensional networks: ice, KH_2PO_4.

In Section 2 experimental methods which contribute to the knowledge of the proton migration are discussed. Section 3 contains a survey of the more important materials for which proton migration has been claimed.

2. Experimental methods

2.1. *Determination of the transport number*

In order to establish or to examine proton migration in solids, several methods have been suggested in the literature. One method is to determine the transport number of protons by means of the electrolysis of the solid. In most cases this was performed in an equipment developed earlier by Schmidt [14]. In this equipment a single crystal or pressed pellet is electrolysed between mercury electrodes. The evolution of hydrogen gas is observed from the movement of cathodic mercury in a capillary, while a sufficiently high voltage is applied to the specimen to provide a sufficiently large charge transport. Comparison of the total amount of hydrogen evolved with the theoretical Faradaic amount would give a value of the transport number.

In another experimental set-up the sample is electrolysed between platinum electrodes in a closed evacuated system and the hydrogen evolution is measured as an increase of the pressure. The results of electrolysis experiments on various materials are represented in Table 1.

Serious objections can be raised against this method. The high voltage usually applied to the specimen principally enables each ion to move. So in this case one must be sure of all *anodic* and *cathodic* electrode reactions that can occur. In none of the electrolysis experiments described in Table 1 have all of these reactions been checked. The evolution of hydrogen gas in exactly the Faradaic amount is no unambiguous proof of protonic conduction as can be easily demonstrated for KHF_2. One can formulate an electrolysis mechanism in which the F^- is mobile and the proton is not, although hydrogen is evolved at the cathode on passage of current.

A better approach is the determination of the transport number by EMF measurements [18, 2]. In these experiments different hydrogen pressures are applied on both sides of the specimen, which are covered by suitable hydrogen electrodes like platinum. The quotient of the measured EMF and that given by Nernst's law is the desired ionic transport number. It should be pointed out, however, that the information contained in the transport number is not equivalent to that determining the proton migration in an electric field.

The only unambiguous experiment to demonstrate whether a material is a proton conductor is the electrolysis of a specimen between two specific hydrogen electrodes. The condition is that the amount of hydrogen consumed at the anode on current passage is equal to the amount of hydrogen developed at the anode. The correspondence between the activation energy for conduction and the activation energy for proton jumps obtained from N.M.R. experiments also provides a good indication [46]. Also tritium diffusion experiments offer a good method for the determination of proton diffusion coefficients [9,50]. Moreover most materials examined are hydrated or sensitive to moisture and very large errors due to surface conduction can be expected. This surface conduction can be eliminated by means of a three-electrode system. Although no unambiguous proof of proton conduction has been given for most of the so-called proton conductors they will be treated as such in the remaining sections. In some situations chemical feeling rather than exact experiments suggests proton conduction as major diffusion mechanism.

2.2. *d.c. conduction measurements*

d.c. conduction measurements on proton conductors are frequently reported in the literature [5, 6, 8, 11, 39]. Generally, the conductivity is calculated from the voltage over and the current through the sample. Usually a decay of the current due to electrode polarization is observed. To solve this problem the constant value of the current after decay is taken as the right one. However, the difference between the applied voltage and the voltage over the specimen due to electrode polarization is ignored and large errors are possible. The only way to overcome this problem is to use reversible proton injecting electrodes [2].

2.3. *a.c. measurements*

This technique is sometimes used to avoid electrode polarization. Although in this field extreme care must be practised, the check on the frequency dependence of the conductivity is not reported in some papers. At lower frequencies polarization effects occur [29], whilst at higher frequencies other relaxation processes often contribute to the impedance. Also, another typical frequency-dependent phenomenon due to a microscopically uneven current distribution has been observed [41].

2.4. *Hall-effect*

A useful technique to measure proton mobilities is provided by Hall-effect measurements. The first Hall-effect measurement in connection with protons was carried out by Bullemer and Riehl on single crystals of ice [35]. The importance of the use of guard-electrodes to separate bulk- and surface-currents has been demonstrated.

Table 1. The determination of the protonic transport number on various materials. p.p.: pressed pellets; s.c.: single crystals

Material	*Specimen*	*Proton current efficiency*	*References*	*Method*
$Li_2SO_4 . H_2O$	p.p.	20±5%	[5]	electrolysis
Borax	p.p.		[6]	electrolysis
Borax	p.p.	5–30%	[7]	electrolysis
$LiN_2H_5SO_4$	s.c.	100%	[8, 12]	electrolysis
$NH_4H_2PO_4$	s.c. + pellets	93%	[9, 2]	electrolysis
$NH_4H_2PO_4$	s.c.	60–140%	[10]	electrolysis
KHF_2	p.p	100±10%	[4]	electrolysis
Imidazole	s.c.	28%//a-axis; 90%//c-axis	[11]	electrolysis
Imidazole	p.p	90–98%	]12]	electrolysis
NH_4ClO_4	p.p.	100%	[13]	electrolysis
Cellulose	p.p.	100%	[19]	electrolysis
KH_2PO_4	s.c.	100%	[14]	electrolysis
Ice	s.c.	95–100%	[15, 16]	electrolysis
Solid cetyl alcohol	p.p.	90%	[17]	electrolysis
Polyamides		80°C electronic 100°C *c.* 50%	[23]	electrolysis
Ice	s.c.	100%	[18]	E.M.F.
NH_4Cl	s.c.	0–60%*	[2]	E.M.F.

*Depends on experimental circumstances.

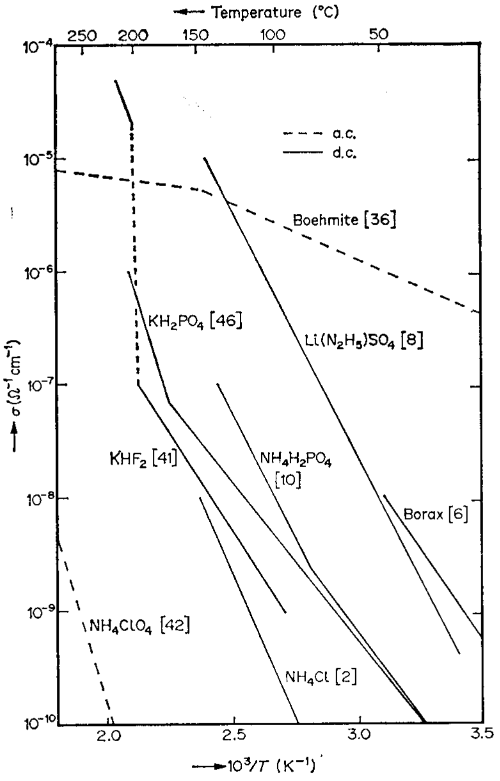

Fig. 1. Conductivities of some proton conductors: ---- a.c.; —— d.c.

A positive sign of the Hall-coefficient was found whilst the mobility decreases with increasing temperature. A simple model was proposed, which characterizes the conductivity mechanism in terms of the time correlated proton jumps across several H-bonds, the time between consecutive jumps, and the effective mass. Application of this technique to other protonic conductors would produce more information on the mechanism of proton conduction.

2.5. *P.M.R.*

Proton magnetic resonance offers a good opportunity to study proton jumping and other important processes in solid proton conductors. The information is useful in explaining the mechanism of the electrical conductivity. In the case of KD_2PO_4 there is a striking correspondence between the activation energy for conduction and the activation energy for deuteron jumps between different D-bonds obtained from N.M.R. studies [46, 48]. In connection with electrolysis experiments a good indication is obtained that the deuteron is indeed the mobile species in KD_2PO_4. Continued rotating frame and dipolar proton spin-lattice relaxation

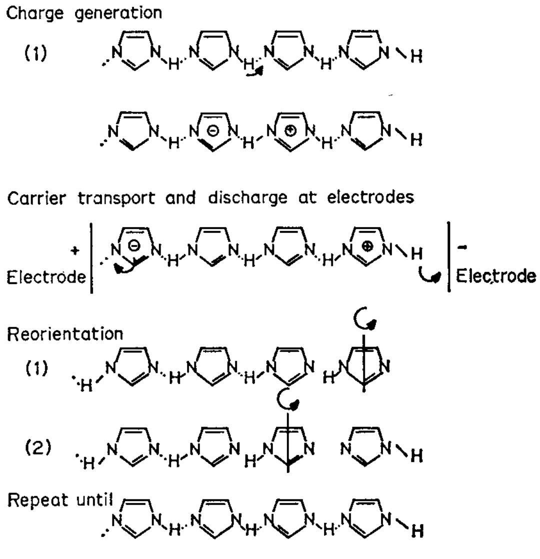

Fig. 2. Charge carrier generation and transport in imidazole. (Courtesy of *J. Chem. Phys.*, **52** (1970) 3124.)

measurements reveal that a slow reorientational process dominates the d.c. protonic conductivity in KH_2PO_4 [38].

3. Proton conduction in solids

Proton conductors can be roughly divided in two groups: organic and inorganic compounds. Although there is a tremendous variety of organic compounds in which hydrogen bridging occurs, yet in only a few of them has proton conduction been demonstrated. In general the conductivity of the organic proton conductors are orders of magnitude less than those of the inorganic ones. (See Fig. 1.)

3.1 *Organic materials*

Imidazole. In solid imidazole the molecules form linear hydrogen bonded chains along the c-direction. Kawada *et al.* found the d.c. conductivity of imidazole to be highly anisotropic [11]; the ratio of conductivity in the c and a crystallographic directions is $\sim 10^3$. These d.c. measurements were performed with two sets of guarded electrodes. The proposed mechanism is represented in Fig. 2.

The rate-determining process in imidazole was suggested to be the reorientation of the imidazole molecule with a large activation energy of 39·5 kcal/mol. In the a direction no extended hydrogen network exists; the conduction mechanism is probably electronic.

Solid alcohols. a.c. measurements at 560 Hz on solid alcohols reveal that the conductivity of long chain compounds decreases considerably with increasing carbon number [17]. This is explained by a mechanism in which a proton transfer is succeeded by the rotation of the acceptor molecule. After that rotation the proton is transferred to the next molecule.

Polyamides. In a detailed study of proton migration in solids, Seanor [23] determined the transport number of protons in polyamides (Table 1).

Organic acids. d.c. conduction measurements on several organic acids were performed by Pollock and Ubbelohde [25]. These measurements were carried out on polycrystalline pressed pellets. No detailed information about polarization effects is given. The results are interpreted as being due to proton migration, which up to now has not been demonstrated.

Table 2 shows that isolated acid dimers, bonded to each other by van der Waals' forces, as in benzoic or furoic acid, have a large activation energy of conduction when compared to ionic crystals. It was suggested that proton transfer via hydrogen bonded water is easier than in absence of water. Moreover, proton migration was believed to be easier in *spiralized* structures such as acetylene dicarboxylic acid.

Sucrose. Proton migration was supposed to take place along lattice defects in sucrose [26]. The injection of protons at a palladium anode saturated with H_2 resulted in a roughly thousandfold increase in the conductivity as compared with Au/N_2 electrodes. The conductivity at room temperature was reported to be 3×10^{-14} $\Omega^{-1}\,cm^{-1}$.

3.2. *Inorganic materials*

Ice. Ice is probably the best known inorganic proton conductor, [15, 16, 18]. Studies on ice have gone on for more than 50 years and a

Table 2. Activation energies and conductivities $\sigma = \sigma_0 e^{-E_a/kT}$ of solid organic acids

Acid	*Activation energy* E_a (kcal . mol^{-1})	(50°C) (Ω^{-1} cm^{-1})
Acetylene dicarboxylic acid dihydrate	6·5	$3{\cdot}5 \times 10^{-6}$
Acetylene dicarboxylic acid (dehydrated)	12·3	$7{\cdot}1 \times 10^{-7}$
Oxalic acid dihydrate	23·5	$2{\cdot}2 \times 10^{-8}$
Oxalic acid (dehydrated)	40·5	$1{\cdot}1 \times 10^{-9}$
Benzoic acid	48·9	$1{\cdot}8 \times 10^{-9}$
Furoic acid	68·4	$1{\cdot}8 \times 10^{-8}$

tremendous number of conduction and polarization studies have been carried out. In ice each oxygen is tetrahedrally surrounded by four neighbours, whilst all oxygen atoms participate in hydrogen bonds. Since no conduction can occur in a perfect lattice two types of defects were postulated [28]: (a) *Ion-states* H_3O^+ *and* OH^-. The oxygen is surrounded by three respectively three and one hydrogen atoms, in contrast with the normal situation in which it is directly bonded to two hydrogen atoms. (b) *Rotational defects D and L.* Between two oxygens there are respectively two and no hydrogen atoms situated, which are involved in direct bonding to the oxygen.

Steineman and Gränicher [28] postulated a double well model to explain the dielectric relaxation phenomena. For instance in the case of rotational defects with formation energy E_0, Fröhlich's general dynamic theory applied to these imperfections gives as a relaxation time:

$$\tau(T) = A\, e^{(\frac{1}{2}E_0 + E_{\mathrm{ROT}})/kT}$$

E_0 = energy of defect formation,

E_{ROT} = activation energy for rotation.

A similar formula is valid for translational relaxation. The relaxation time for pure ice was shown to depend exponentially on the temperature, with an activation energy equal to the sum of the energies for both the formation and migration of lattice defects. The introduction of a sufficient amount of HF into ice leads to the formation of L-defects. Then the energy of rotation can be eliminated from the formula for the relaxation. Small amounts of HF in ice result in the creation of ionic defects as majority carriers by the reaction $HF + H_2O \rightarrow H_3O^+ + F^-$. The results of conductivity measurements on pure and doped ice were discussed by means of the defects mentioned earlier [29, 30]. The main principle in the explanation of the mechanism of the conduction is the initial transfer of majority carriers along a chain of hydrogen bonds, resulting in a blocking of this path for defects of the same sort. Defects of the other sort reactivate this path. In spite of the large number of investigations, no general agreement has been obtained [31]. In three recent papers Von Hippel *et al.* point out serious objections to most of the theories and experiments [32, 33, 34].

In a new interpretation of the intrinsic polarization phenomena, they regard the L,D-pair formation as a one-step process, in which the proton is shifted by a near-infrared phonon to an empty corner of its H_2O tetrahedron. Ionic defects are not able to transfer charge from one electrode to the other. If they move down-stream, the anti-polarization created by this intermolecular proton transfer pumps the corresponding charge upstream. In this case Von Hippel did suggest that only L,D-defects carry charge through an ideal ice crystal. Interconversion of L,D defects and ionic defects was proposed to take place at the electrodes, in order to explain d.c. conductance. However, we think that this model still does not explain the continued electrolysis. In their experiments Madique and Von Hippel [34] proved the high activation energy of conductivity often found in the literature (~ 33 kcal/mol) to be caused by surface conduction as was already pointed out by Bullemer [35]. Initial currents are characterized by zero activation energies. Intermediate values are caused by apparent conductivities in fields distorted by space charge. The conductivity of pure ice measured with a guard technique was at $-10°C$: $1{\cdot}5\times10^{-10}\ \Omega^{-1}\ cm^{-1}$. Our final conclusion is that conduction experiments with proper hydrogen injecting electrodes have not been done up till now.

Boehmite. Another solid in which proton migration is believed to be present is boehmite (γ-AlOOH). In this solid an OH—O zig-zag occurs which has some correspondence with the structure of ice. However, in boehmite the existence of D- and L-defects is less probable because of the high repulsion of the protons in a D-position. Therefore, the well-marked dielectric absorption was explained as a Debye relaxation of ion pairs [36]. This dielectric absorption was found to be superimposed on conduction. The ion pair defects in boehmite are probably generated by tunnelling of a proton through the potential energy barrier along the O—O bond. It has previously been established by Fripiat *et al.* by I. R. experiments that this tunnelling probability through the potential barrier along the OH—O chain was close to one at the energy level of 11 kcal . mol^{-1} above the fundamental level [27]. The activation energies for various processes are represented in Table 3 in comparison with those for ice.

Table 3. Activation energies (kcal . mol^{-1}) observed in ice and in boehmite

	Ice	*Boehmite*
Dipolar absorption	13·3	15·7
Conduction	14·1	5·1
Diffusion (tritons or deuterons)	13·5	15·7

Obviously, the activation energy for tritium diffusion is the same as that for the dielectric relaxation. Fripiat *et al.* give a detailed explanation of all observed processes. The measured conductivity of boehmite at 8 kHz is represented in Fig. 1.

$NH_4H_2PO_4$. Ammonium dihydrogenphosphate has a crystal structure in which hydrogen bonds join adjacent PO_4^{3-}-groups [51]. The hydrogen bond structure is formally the same as that of KH_2PO_4. D.C. measurements on single crystals were performed by Murphy [10, 37] by a direct method, i.e. the measurement of current and voltage across the crystal as a whole. Measurements on both doped and pure crystals were reported. The behaviour of conductivity *v.* temperature was best described as:

$$\sigma = \sigma_{01} \exp(-W_1/kT) + \sigma_{02} \exp(-W_2/kT).$$

The results are represented in Table 4.

The conductivities along the a, b and c axes were essentially the same. The average of the activation energy of the conductivity of doped crystals, i.e. 10 · 5 kcal . mol^{-1}, is taken to be the activation energy for migration, whilst from the conductivity data for the pure crystals the energy required for the formation of defects is calculated to be 19·8 kcal . mol^{-1}. These defects can be formed by the transference of a proton between neighbouring $(H_2PO_4)^-$ groups, the products being an excess and a defect proton. The excess and defect proton are supposed to migrate through the lattice by tunnelling between states of equal energy. The configurations of the hydrogen bonds are continually changing locally due to the breaking of the hydrogen bonds by thermal agitation. The relaxation time required by groups adjacent to a given ion to reach a configuration favourable to tunnelling of the proton is characterized by an activation energy of 10·5 kcal . mol. A.C. conductivity studies as function of temperature with $NH_4H_2PO_4$ have been carried out by

Table 4. Values of W_1, W_2 and σ_{01}, σ_{02} for conduction in single crystals of $NH_4H_2PO_4$ (kcal . mol^{-1}, Ω^{-1} cm^{-1})

Author	*Type of conduction*	*Conc.* M%	W_1*(kcal . mol^{-1})*	W_2	σ_{01}	$\sigma_{02}(\Omega^{-1}\ cm^{-1})$
Murphy	Intrinsic		20·4	14·4	65×10^3	1·5
	Impurity Ba^{2+}	0·004		10·1		$6{\cdot}2\times10^{-2}$
	SO_4^{2-}	0·006		10·9		$4{\cdot}4\times10^{-2}$
Pollock	extrinsic ?	?		11·08		$1{\cdot}26\times10^{-2}$

Pollock and Sharan [9]. These resulted in a single straight line with about the same slope as mentioned by Murphy for the case of doped material. Pollock and Sharan explained the absence of a 'knee' in the log σ v. T^{-1} plot by the assumption that defect formation and migration are the same process. However, their measured conductivity appears to be about two orders of magnitude larger than that measured by Murphy. A simple explanation is that their crystals contain large amounts of impurities.

KH_2PO_4. The crystal structure of potassium hydrogen phosphate is somewhat similar to that of ice. In KH_2PO_4 the hydrogen bonds lie approximately in a plane normal to the c axis of the tetragonal crystal [Fig. 3]. Two of these bonds are from oxygens on the upper side of the PO_4 tetrahedron to oxygens on the lower side of neighbouring PO_4 groups. The other two bonds are associated with the two lower oxygens of the PO_4 tetrahedron and join with upper oxygens of neighbouring groups. The defect formation as proposed by O'Keeffe and Perrino [46] is shown in Fig. 3B: a chain of M defects terminate in an L and D defect. An M defect is a configuration of higher energy in which one proton is associated with an upper oxygen and one with a lower oxygen. The nomenclature of L and D defects is analogous with that used in ice. In Fig. 3C the formation and migration of protonic defects are represented.

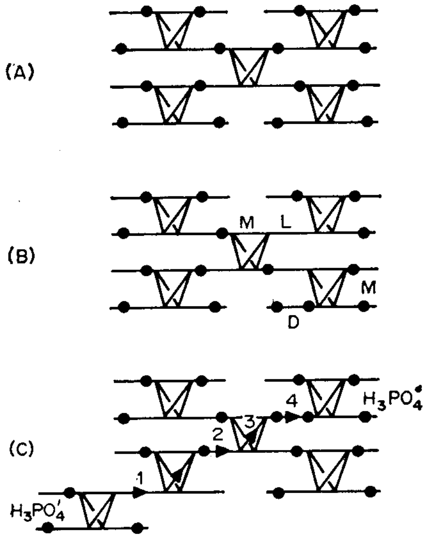

Fig. 3. Proton configurations in KH_2PO_4. The horizontal lines represent hydrogen bonds between PO_4 tetrahedra; the small filled circles represent hydrogen atoms. The diagram represents appoximately a projection on the (110) plane. (A) in perfect ferroelectric KH_2PO_4; (B) crystal with a chain of M defects terminating in an L and a D defect; (C) formation of an ion pair followed by migration of $H_3PO_4^{\cdot}$. The numbered arrows represent a possible sequence of jumps in going from the perfect crystal (A) to the final situation shown. (Courtesy of *J. Phys. Chem. Solids*, **28** (1967) 213.)

The subsequent steps are:

(1) $2H_2PO_4 \rightarrow (HPO_4', H_3PO_4^{\circ})$
(2) $(KPO_4', H_3PO_4^{\cdot}) + H_2PO_4 \rightarrow HPO_4' + (H_2PO_4, M) + H_3PO_4^{\cdot}$
(3) $(H_2PO_4, M) \rightarrow H_2PO_4 + L + D$
(4) $H_3PO_4^{\cdot} + H_2PO_4 \rightarrow (H_2PO_4, M) + H_3PO_4^{\cdot}$
(5) $D + (H_2PO_4, M) \rightarrow H_2PO_4 + D$
or $L + (H_2PO_4, M) \rightarrow H_2PO_4 + L$.

Steps 1–3 are only of importance in the case of higher temperatures and/or impure materials. Steps 4–5 describe the migration process. The conductivity of KH_2PO_4 appeared to be isotropic and is for pure crystals given by

$$\log \sigma = -0{\cdot}89 - 12{\cdot}65/2{\cdot}3RT \quad T < 180°C$$

$$\log \sigma = 2 - 18{\cdot}0/2{\cdot}3RT \quad T > 180°C$$

The room temperature conductivity was found to be a linear function of sulphate concentration. The substitution of HSO_4^- for H_2PO_4 creates an L defect; the migration of this defect controls the conductivity. Independently Blinc and Pirš found by means of N.M.R. that slow rotation of H_2PO_4 dominates the conduction process [38]. With a known amount of dopant it is possible to calculate the mobility of an L defect: $\mu_L = 6 \times 10^{-10}$ cm^2 V^{-1} s^{-1}. The higher temperature conductivity reflects the simultaneous thermal generation of ions and D, L defects by steps 1–3, and their simultaneous migration. The activation energy for formation and migration of an ion pair is thus found to be 5·4 kcal . mol^{-1}. The conductivity of KH_2PO_4 was also reported by Harris and Vella [39], who found roughly the same behaviour. However, they did not mention precisely the amount and character of the dopants. Bradley *et al.* [40] measured the conductivity at 1592 Hz as a function of temperature and pressures up to 60 kbar. The value of the activation energy decreases slightly with increasing pressure, whereas σ_0 is virtually constant. The pressure dependence gives an overall activation volume of $-1{\cdot}1$ cm^3 mol^{-1}. The activation energy when extrapolated to low pressure (13·1 kcal . mol^{-1}) is in good agreement with that of O'Keeffe at $T < 180°C$. This single activation energy is explained by the fact that at higher pressures the proton will occupy a position midway between bonded atoms. Thus the energy of formation of the anion pair would decrease. However, impure material should show the same behaviour.

KHF_2. In potassium hydrofluoride, the hydrogen is symmetrically located inside isolated $(FHF)^-$ dumb-bells. KHF_2 has a phase transition at 196°C. In the tetragonal unit cell of KHF_2, stable below the transition point, the F-H-F units are arranged in planes perpendicular to the c-axis. In the cubic phase these units are directed parallel to either one of the four body diagonals. Pollock and Sharan performed a.c. conductivity measurements on polycrystalline pellets at 1592 Hz [4]. They observed a large enhancement of the conductivity at the transition point. The suggested mechanism of conduction through the crystals is by migration of interstitial protons or 'proton defects'. It was suggested that the observed activation energies refer to the formation of these defects (Table 5).

A large discrepancy can be observed in their reported values of activation energies and those computed from their graphs. Bradley *et al.* [40] made conduction studies in KHF_2 at various pressures; the activation volume being 2·5 cm^3 mol^{-1}. They concluded that the activation volume of proton conduction is remarkably small. a.c. impedance measurements in the range 50 Hz–10 kHz have been made in KHF_2 pressed pellets and single crystals by Bruinink and Broers [41]. These experiments underline the importance of controlled environmental conditions i.e. an HF pressure. This fact was ignored by previous investigators.

The admittance of KHF_2 single crystals and pressed pellets is frequency dependent and can be represented by a parallel combination of a capacitance $C(\infty)$, a conductance $G(0)$ and a Warburg admittance $Y_W(\omega) = (1+j)k\omega^{\frac{1}{2}}$. The temperature dependence of $G(0)$ for the low temperature α-phase is very much different for pressed pellets and single crystals. The polycrystalline specimens show a large specific conductivity σ (0) as well as a stronger temperature dependence. The difference is caused by a predominant contribution of surface conduction in polycrystalline materials, which also explains the scattered results of previous investigators. Bulk conduction prevails in single crystals. The zero frequency conductivity σ (0) of single crystals does not show any detectable anisotropy and was found to be identical with the d.c. conductivity. No definite proof has been given that protons are indeed the mobile charge carriers in KHF_2.

NH_4ClO_4. The electrical conductivity of solid ammonium perchlorate was measured both with single crystals and pressed pellets and did not show any discontinuity when going from the ortho-rhombic to the cubic crystal structure [42]. The conductivity was found to be dependent of the partial ammonia pressure of the surrounding atmosphere and to be equal for single crystals and pressed pellets. The conduction mechanism proposed was that of a Grotthus mechanism: the movement of a proton from an

Table 5. Activation energies of conduction in kcal . mol^{-1} of polycrystalline samples and single crystals of KHF_2

Authors	*Pollock and Sharan (Fig. 2)*	*Pollock and Sharan (reported)*	*Bradley*	*Bruinink and Broers*	
				p.c.	*s.c.*
Freq. Hz.	1592	1592	1592		
p.c.	15·6	21·7	11–12	29–31	17±1·5
p.c.	18·7	19·8		19·7	20·5±1·5

ammonium ion to an ammonia molecule at a lattice vacancy or interstitial. Such a model appears to explain the increase in electrical conductivity encountered in the presence of ammonia. Application of the usual theory of defect formation yields: 20 kcal . mol^{-1} as the energy barrier for proton migration and 24 kcal . mol^{-1} for the enthalpy of defect formation.

NH_4Cl. d.c. conductivity measurements on pure and doped single crystals of ammonium chloride have been carried out by Herrington and Staveley [43]. It was assumed that there was no electronic conductance. The measured conductivity is much greater than that for comparable alkali halides. The proposed mechanism was:

(1) A proton switch from the NH_4^+-ion to a chloride adjacent to a vacancy ($NH_4^+ \rightarrow NH_3 + HCl$.
(2) Migration of one of the molecules into the vacancy.
(3) Reverse proton switch to reform pair of ions.

The activation energy for migration was found to be: 17·2 kcal . mol^{-1}, that for formation of defects: 18·4 kcal . mol^{-1}. Later on, Fuller and Patten [44] measured the conductivities of NH_4Cl and ND_4Cl. They concluded from their measurements that the proton was indeed the mobile species and found an activation energy for migration of 3·5 kcal . mol^{-1} and an energy of defect formation of 51 kcal . mol^{-1}.* To examine what are in fact the mobile species in NH_4Cl, Kröger has carried out EMF measurements on NH_3, H_2 gas concentration cells with NH_4Cl as solid electrolyte [2]. The transport numbers found: $t_{H^+} = 0$–0·47, ${}_{NH_4^+} = 0{\cdot}23$–1, $t_{el} = 0$–0·35 depend on the composition of the gas mixture used. The general behaviour of σ as $f(T^{-1})$ was found to be similar to that observed by Herrington and Staveley. In general the conductivities did not vary significantly with the composition of the gas phase. Kröger interpreted the results to be dependent on defect concentrations of protonic, NH_4^+, Cl^- and electronic defects.

$Li(N_2H_5)SO_4$. The d.c. electrical conductivity of lithium hydrazinium sulphate single crystals was found to be remarkably anisotropic with the direction of easiest conduction along the c axis [8]. The absolute values of the conductivity in the directions of the crystallographic axes at 25·5°C were determined to be:

a axis $\sigma_{dc} = 0{\cdot}93 \pm 0{\cdot}09 \times 10^{-11}\ \Omega^{-1}\ \mathrm{cm}^{-1}$
b axis $= 0{\cdot}80 \pm 0{\cdot}09 \times 10^{-11}$
c axis $= 0{\cdot}23 \pm 0{\cdot}09 \times 10^{-8}$.

The conductivity along the c axis was found to obey

$$\sigma_{dc} = 49 \times 10^4 \exp(-19{\cdot}6/kT)\ \Omega^{-1}\ \mathrm{cm}^{-1}$$

However some serious difficulties concerning polarized electrodes were involved and a large discrepancy with a.c. measurements was observed. In solid $Li(N_2H_5)SO_4$ the hydrazinium ions are located in channels formed by oxygen tetrahedrons, and are linked by hydrogen bonds between their $-NH_2$ groups, thus forming infinite chains. The existence of these chains was thought to be responsible for the transfer of protons along the hydrogen bond and thus for the conductivity along the c axis.

Borax. $Na_2B_4O_5(OH)_4 \cdot 8H_2O$. The crystal structure of borax can be characterized by continuous chains of hydrogen bonded B_4O_5-rings running parallel to the c direction. Each of these chains is neighboured by four channels of Na^+ ions. There are also hydrogen bonds along the b direction between the anionic part of the structure and the water molecules in the cationic channels. d.c. measurements reveal the absolute value of the conductivity along the b axis as three orders of magnitude larger than for that along the sin β and c directions [6]. A minimum temperature (~ 21°C) is observed below which proton conduction ceases. This effect was discussed in relation to the competition between the reorientation rate of protons and their concentration.

The dielectric behaviour of compressed powder and single crystals over an extensive range of frequencies and temperatures is described by

---

* The origin of the large difference between the activation energies can probably be explained by undefined impurities and/or aggregates in the specimens used by Herrington and Staveley.

Giesekke and Glasser [45]. In powder samples two dielectric absorptions are observed: a low-frequency absorption due to space-charge polarization and a higher frequency absorption arising from the reorientation of water molecules absorbed on the surfaces of the powder particles. Furthermore these effects were found to be strongly dependent on the ambient humidity and the age of the powder; single crystals appear to be less sensitive to external conditions.

$Li_2SO_4 . H_2O$. By employing a palladium–hydrogen electrode, Thomas and Clarke measured the conductivity of lithium sulphate monohydrate [47]. They found that proton conduction is favoured only along the b axis, in which direction a continuous zig-zag pattern of regularly oriented water molecules occurs. The conductivity yields an activation energy of 20 ± 1 kcal mol^{-1}. From current-voltage characteristics the effective mobility was estimated to be *c.* 10^{-7} to 10^{-8} $cm^2\ V^{-1}\ s^{-1}$. From an examination of the structure of the solid Thomas and Clarke formulated a mechanism, based on Grotthus conduction, for the migration of protons. In the case of borax, N.M.R. experiments have shown that the rate-determining process for conduction is the reorientation of a water molecule in the conductive chain [49].

4. Conclusions

Finally we reach the following conclusions. In most of the so-called proton conductors no unambiguous proof of proton conduction has been given. Therefore the development of a proper method to demonstrate proton conduction would be of great value. Some of the reported conduction experiments are open to some doubt. In the case of d.c. experiments this is due to the use of improper electrodes, whereas in a lot of a.c. experiments no check of frequency dependence is reported. Especially in hydrated materials like borax large surface currents can occur, which must be eliminated carefully by guard ring techniques. For a useful application in H_2–O_2 fuel cells, efforts must be directed to finding fast proton conducting materials, which are insoluble in and do not react with water.

Acknowledgement

The author gratefully acknowledges profitable discussions with Prof. Dr W. van Gool and Dr G. H. J. Broers. These studies were part of a research project supported by NATO (Grant No. 475).

References

[1] A. F. Wells, 'Structural Inorganic Chemistry', 3rd. ed. Oxford (1962).

[2] F. A. Kröger, *J. Chem. Phys.*, **51,** (1969) 4025.

[3] M. Christen, 'Diffusion des protons dans les solides'. Centre de Recherche de la C.G.E. Marcoussis, France.

[4] J. M. Pollock and M. Sharan, *J. Chem. Phys.*, **47,** (1967) 4064.

[5] S. Maričic, V. Pravić and C. Veksli, *Croat. Chim. Acta*, **33** (1961) 187.

[6] S. Maričic, V. Pravić and C. Veksli, *J. Phys. Chem. Solids*, **23** (1962) 1651.

[7] E. W. Giesekke, and L. Glasser, *J. Phys. Chem.*, **71** (1967) 2573.

[8] J. van der Kooy, J. D. Cuthbert and H. E. Petch, *Can. J. Phys.*, **42** (1964) 1871.

[9] J. M. Pollock and M. Sharan, *J. Chem. Phys.*, **51** (1969) 3604.

[10] E. J. Murphy, *J. Appl. Phys.*, **35** (1964) 2609.

[11] A. Kawada, A. R. McGhie and M. M. Labes, *J. Chem. Phys.*, **52** (1970) 3121.

[12] R. Chan-Henry and L. Glasser, National Symp. on Electrochem., Pretoria, April 1970.

[13] V. V. Boldyrev and E. F. Khairetinov, *J. Inorg. Nucl. Chem.*, **31** (1969) 3332.

[14] V. H. Schmidt, *J. Sci. Instrum.*, **42** (1965) 889.

[15] E. J. Workman, F. K. Truby and W. D. Hansen, *Phys. Rev.*, **94** (1954) 1073

[16] J. C. Decroly, H. Gränicker and C. Jaccard, *Helv. Phys. Acta*, **30** (1957) 465.

[17] Y. Kakiuchi, H. Komatsu and S. Kyoya, *J. Phys. Soc. Japan*, **6** (1951) 321.

[18] P. N. Krishnan, I. Young and R. E. Salomon, *J. Phys. Chem.*, **70** (1966) 1595.

[19] E. J. Murphy, *Can. J. Phys.*, **41** (1963) 1022.

[20] H. Zimmerman, *Ber. Bunsenges. Physik. Chem.*, **63** (1959) 601.

[21] N. Joop and H. Zimmerman, *Ber. Bunsenges. Physik. Chem.*, **66** (1962) 440.

[22] N. Riehl, *Naturwissenschaften*, **43** (1956) 145.

[23] D. A. Seanor, *J. Polym. Sci.*, **A2, 6** (1968) 463.

[24] M. E. Baird, *J Polym. Sci.*, **A2, 8** (1970) 739.

[25] J. M. Pollock and A. R. Ubbelohde, *Trans. Far. Soc.*, **52** (1956) 1112.

[26] J. M. Thomas and J. O. Williams, *Chem. Comm.*, **1968,** 209.

[27] J. J. Fripiat, H. Bosmans and P. G. Rouxhet, *J. Phys. Chem.*, **71** (1967) 1097.

[28] A. Steinemann and H. Gränicker, *Helv. Phys. Acta*, **30** (1957) 553.

[29] H. Gränicker, C. Jaccard, P. Scherrer and A. Steinemann, *Disc. Far. Soc.*, **23** (1957) 50.

[30] C. Jaccard, *Helv. Phys. Acta*, **32** (1959) 89.

[31] I. G. Young and R. E. Salomon, *J. Chem. Phys.*, **48** (1968) 1635.

[32] A. von Hippel, D. B. Knoll and W. B. Westphal, *J. Chem. Phys.*, **54** (1971) 134.

[33] A. von Hippel, *J. Chem. Phys.*, **54** (1971) 150.

[34] M. A. Madique, A. von Hippel and W. B. Westphal, *J. Chem. Phys.*, **54** (1971) 150.

[35] B. Bullemer and N. Riehl, *Phys. Kondens. Materie*, **7** (1968) 248.

[36] A. M. Arjona and J. J. Fripiat, *Trans. Far. Soc.*, **63** (1967) 2936.

[37] E. J. Murphy, *Ann. of New York Ac. of Science*, **118** (1965) 727.

[38] R. Blinc and J. Pirs, *J. Chem. Phys.*, **54** (1971) 1535.

[39] L. B. Harris and G. J. Vella, *J. Appl. Phys.*, **37** (1966) 4294.

[40] R. S. Bradley, D. C. Munro and S. I. Ali, *J. Inorg. Nucl. Chem.*, **32** (1970) 2513.

[41] J. Bruinink and G. H. J. Broers, *J. Phys. Chem. Solids*. To be published.

[42] H. Wise, *J. Phys. Chem.*, **71** (1967) 2843.

[43] T. M. Herrington and L. A. K. Staveley, *J. Phys. Chem. Solids*, **25** (1964) 921.

[44] R. G. Fuller and F. W. Patten, *J. Phys. Chem. Solids*, **31** (1970) 1539.

[45] E. W. Giesekke and L. Glasser, *J. Phys. Chem.*, **71** (1967) 2573.

[46] M. O'Keeffe and C. T. Perrino, *J. Phys. Chem. Solids*, **28** (1967) 211.

[47] J. M. Thomas and T. A. Clarke, *Trans. Far. Soc.*, **65** (1969) 2718.

[48] V. H. Schmidt and E. A. Uekling, *Phys. Rev.*, **126** (1962) 447.

[49] M. I. Valic and M. M. Pintar, *Phys. Stat. Sol.*, **42** (1970) 661.

[50] P. Hoffmann and K. H. Lieser, *Zeitschrift für Physikalische Chemie N.F.*, **68** (1969) 1.

[51] J. C. Slater, *J. Chem. Phys.*, **9** (1941) 16.